Proplatelet formation is regulated by the Rho/ROCK pathway

Yunhua Chang,[1,2,6] Frédéric Auradé,[1,2,6] Frédéric Larbret,[2,6] Yanyan Zhang,[1,2,6] Jean-Pierre Le Couedic,[1,2,6] Laurence Momeux,[3] Jerôme Larghero,[4] Jacques Bertoglio,[5] Fawzia Louache,[1,2,6] Elisabeth Cramer,[3] William Vainchenker,[1,2,6] and Najet Debili[1,2,6]

[1]Institut National de la Santé et de la Recherche Médicale (INSERM), Unité (U) 790, Pavillon de Recherche 1, Institut Gustave Roussy, Villejuif, France; [2]Université Paris XI, Institut Fédératif de Recherche (IFR) 54, Institut Gustave Roussy, Villejuif, France; [3]INSERM, U567, Institut Cochin, Département d'Hématologie, Paris, France; [4]Laboratoire de Therapie Cellulaire, Hôpital Saint-Louis, Paris, France; [5]INSERM, U749, Faculté de Pharmacie, Chatenay-Malabry, France; [6]Institut Gustave Roussy, Villejuif, France

Platelets are released by megakaryocytes (MKs) via cytoplasmic extensions called proplatelets, which require profound changes in the microtubule and actin organization. Here, we provide evidence that the Rho/ROCK pathway, a well-known regulator of actin cytoskeleton, acts as a negative regulator of proplatelet formation (PPF). Rho is expressed at a high level during the entire MK differentiation including human CD34$^+$ cells. Thrombopoietin stimulates its activity but at a higher extent in immature than in mature MKs. Overexpression of a dominant-negative or a spontaneously active RhoA leads to an increase or a decrease in PPF indicating that Rho activation inhibits PPF. This inhibitory effect is mediated through the main Rho effector, Rho kinase (ROCK), the inhibition of which also increases PPF. Furthermore, inhibition of Rho or ROCK in MKs leads to a decrease in myosin light chain 2 (MLC2) phosphorylation, which is required for myosin contractility. Interestingly, inhibition of the MLC kinase also decreases MLC2 phosphorylation while increasing PPF. Taken together, our results suggest that MLC2 phosphorylation is regulated by both ROCK and MLC kinase and plays an important role in platelet biogenesis by controlling PPF and fragmentation. (Blood. 2007;109:4229-4236)

Introduction

Megakaryocytes (MKs) are the highly specialized precursor cells that lead to platelet production. MK differentiation is a continuous process characterized by sequential steps.[1] First, MKs increase their ploidy via endomitosis and begin to increase their size.[2] Then, the synthesis of storage organelles is enhanced, as well as the synthesis of plasma membrane to form the demarcation membranes. This cytoplasmic maturation is associated with a marked increase in the MK size. Finally, mature MKs release platelets probably through cytoplasmic fragmentation at the tips of long and thin extensions called proplatelets (PPTs) that contain all the platelet organelles.[3,4] The mechanisms controlling proplatelet formation (PPF) are still incompletely understood. However, PPF is associated with remarkable morphologic changes that require a profound reorganization of the cytoskeleton.[5] Increasing evidence indicates that PPTs arise from the unfolding of demarcation membranes. The microtubule cytoskeleton provides the sliding power to unfold demarcation membranes and thus to induce the pseudopodial elongations corresponding to PPTs.[6] In addition, microtubules permit the organelle transport in the PPTs and maintain the platelet discoid shape.[7-10]

Although not studied in detail, the actin cytoskeleton may also participate in PPF because cytoplasmic polymerized actin is associated with demarcation membranes and actin is highly aggregated in cultured MKs when PPF occurs.[11] In addition, a crucial role of the actin cytoskeleton has been reported in platelet functions since it regulates platelet shape in unstimulated and activated platelets.[12] Evidence suggests that actin cytoskeleton may play important roles during PPT formation at 2 different stages: (1) at early stages, inhibition of actin polymerization blocks PPF before pseudopodial elongation.[11,13] This may be related to a role of actin cytoskeleton in the repartition of demarcation membranes. (2) During PPF, actin cytoskeleton may be involved in branched extensions of linear PPTs and thus may allow an increase in platelet-shedding efficiency.[10] Thus, the actin cytoskeleton may play an important role at both early and late stages of platelet biogenesis.

The Rho GTPase family (about 20 members in humans) works as a molecular switch that controls signal transduction pathways in numerous cellular processes by cycling between an inactive GDP and an active GTP form.[14-16] Rho proteins (RhoA, RhoB, and RhoC), the best characterized members of this family, were initially described for their roles in the dynamics of the actin structure. ROCK is a key Rho effector that phosphorylates myosin light chain 2 (MLC2) at Ser19 and inhibits myosin phosphatase.[17,18] MLC2 phosphorylation is necessary for actin/myosin motor activation to provide essential contractile forces for a diversity of cellular processes, such as cell contraction, cytokinesis, cell migration, and membrane blebbing.[19-21] The Rho/ROCK pathway is implicated in platelet shape changes during activation by mediating MLC2 phosphorylation.[22-25] We have shown previously that MK adhesion to collagen leads to an inhibition of PPF likely through the activation of the Rho/ROCK pathway.[26] Nevertheless, the expression and activation of Rho during MK differentiation as well as the

Submitted April 27, 2006; accepted January 6, 2007. Prepublished online as *Blood* First Edition Paper, January 23, 2007; DOI 10.1182/blood-2006-04-020024.

The publication costs of this article were defrayed in part by page charge payment. Therefore, and solely to indicate this fact, this article is hereby marked "advertisement" in accordance with 18 USC section 1734.

precise role of the Rho/ROCK pathway in PPF remain poorly understood. In this study, we address these issues by using a serum-free liquid culture system. Our results reveal that the Rho/ROCK pathway is a negative regulator for PPF likely through MLC2 phosphorylation.

Materials and methods

In vitro culture of MKs derived from human CD34$^+$ cells in liquid serum-free medium and purification of the CD41$^+$ population

CD34$^+$ cells were obtained, after informed consent in agreement with our Institute Ethic Committee (Assistance Publique des Hôpitaux de Paris) and in accordance with the Declaration of Helsinki, either from leukapheresis samples after mobilization performed on patients or from umbilical cord blood. CD34$^+$ cells were isolated by a positive selection using an immunomagnetic cell sorting system (AutoMacs; Miltenyi Biotec, Bergisch Gladbach, Germany) and were cultured in serum-free medium in the presence of recombinant human thrombopoietin (TPO; 10 ng/mL; Kirin Brewery, Tokyo, Japan). Ingredients used to prepare the serum-free medium were as previously described.[27] To purify the CD41$^+$ population, cells in culture were collected at day 5, stained with an anti–CD41a-PE monoclonal antibody (mAb; PharMingen, San Diego, CA) and purified by cell sorting (FacsDIVA, Becton Dickinson, le Pont de Claix, France). The CD41$^+$ cell population was grown in serum-free medium for an additional 6 to 9 days.

Retroviral plasmid construction and retrovirus production

The active and dominant-negative forms of Rho (RhoAV14 and RhoAN19) were inserted upstream the internal ribosome entry site (IRES) of the murine stem cell virus-internal ribosome entry site-green fluorescence protein (MSCV-IRES-GFP) retrovirus (Migr-GFP). Migr-GFP, Migr-RhoAV14-GFP, and Migr-RhoAN19-GFP retroviruses were produced by 293 EBNA cells cotransfected with 2 other plasmids, pCMV *gag-pol* and pCMV-*VSV-G* (vesicular stomatitis virus envelope glycoprotein; provided by J. Morgenstein, Cambridge, MA) as previously described.[28] Supernatants were collected 48 hours, 72 hours, and 96 hours after transfection, pooled, and concentrated about 100-fold by centrifugation (1000*g*, 1 hour at 4°C) over a Centricon plus-70 (Millipore, MA). Viruses stocks were aliquotted and kept frozen at −70°C. Viruses stocks were thawed freshly used.

MK infection

CD34$^+$ cells isolated from cord blood were cultured 6 days in serum-free medium in the presence of TPO (10 ng/mL; Kirin Brewery) and recombinant human stem cell factor (SCF; 25 ng/mL; Amgen, Thousand Oaks CA). CD34$^+$ cells isolated from leukapheresis were cultured 3 days with TPO, IL-3 (100 U/mL; kindly provided by Novartis, Paris, France), SCF, and FLT3-L (10 ng/mL; Amgen). The cells then were seeded in 24-well plates (500×10^3 cells/well) and infected by adding 100 μL concentrated retrovirus stock and 400 μL serum-free medium with TPO plus SCF for the cells derived from cord blood (day 7) or a cocktail of cytokines for the cells derived from leukapheresis (day 4), as described. A second round of infection was performed 24 hours later by changing fresh medium with cytokines and adding fresh virus. After an additional 24 hours, cells were extensively washed in serum-free medium and stained with an anti–CD41a-PE mAb. The CD41$^+$GFP$^+$ cell population was purified by cell sorting and cultured in serum-free medium in 96 wells in the presence of TPO for 10 to 13 days (MKs derived from leukapheresis) or for 12 to 15 days (MKs derived from cord blood) at which times PPF was scored.

Conventional and confocal microscopy

CD34$^+$ cells isolated from leukapheresis cultured 6 days or 12 days in serum-free medium with TPO or the CD41$^+$GFP$^+$ cell population were plated on slides coated with poly-L-lysine (O. Kindler, Freiburg, Germany) for 1 hour at 37°C with 5% CO_2 in air and 100% humidity. The cells were then fixed in 4% paraformaldehyde for 5 minutes, permeabilized by 0.1% Triton X-100 for 5 minutes, and incubated with different antibodies for 1 hour at room temperature. After 3 washes, the cells were incubated with the appropriate secondary antibodies conjugated with FITC or TRITC (Jackson ImmunoResearch, West Grove, PA) or Alexa 633 (Molecular Probes, Leiden, The Netherlands). TOTO-3 iodide (Molecular Probes) was used for nucleus staining. Cells were examined under a Zeiss laser scanning microscope (LSM 510 Zeiss, Jena, Germany) equipped with a 63 ×/1.4 numerical aperture (NA) oil objective. The following antibodies were used: mouse anti-Rho mAb (Upstate Biotechnology, Lake Placid, NY), mouse anti–phospho-MLC2 Ser19 mAb (pMLC2; Cell Signaling Technology, Beverly, MA), and phalloidin-TRITC and rabbit anti–von Willebrand factor (VWF) polyclonal antibody (Dako, Glostrup, Denmark).

Pull-down assay

Pull-down assays were performed with a Rho activation assay kit (Upstate Biotechnology). The Rho protein signal was detected with a mouse anti-Rho mAb from Pierce Biotechnology (Pierce, Rockford, IL). To analyze Rho activity, CD34$^+$ cells isolated from leukapheresis were cultured 5 days in serum-free medium with TPO and the CD41$^+$ cell population was isolated as described in the first paragraph of "Materials and methods." The CD41$^+$ cell population was then grown in serum-free medium with TPO. One day after (day 6) or 5 days after (day 11), CD41$^+$ MKs were washed twice with serum-free medium and cytokine-deprived overnight. The next day (day 7 or day 12), MKs were stimulated by TPO (100 ng/mL) and collected at times indicated. Cells were washed twice in Tris-buffered saline (TBS) at 4°C and manipulated according to the protocol of the Rho activation assay kit. Pull-down assays were performed with about 2.5×10^6 CD41$^+$ cells at day 7 and day 12.

Western blot analysis

CD34$^+$ cells isolated from leukapheresis were cultured in serum-free medium with TPO and one part of CD34$^+$-drived cells were harvested at day 3. The remaining CD34$^+$ cells were grown with TPO until day 5. At day 5, CD41$^+$ MKs were selected as described in the first paragraph of "Materials and methods" and grown for additional days with TPO. The CD41$^+$ cell population was harvested at different times of culture, washed once in PBS or TBS, lysed in 2 × Laemmli buffer (100 mM Tris, pH 6.8, 20% glycerol, 4% SDS, 0.05% bromophenol blue, and 10 mM DTT) and the lysates were then gently sonicated on ice. Protein concentrations were measured to ensure equal loading among lanes (Bio-Rad Dc protein assay kit, Bio-Rad, Hercules, CA). Samples were boiled 5 minutes in loading buffer and subjected to sodium dodecyl sulfate-polyacrylamide gel electrophoresis (SDS-PAGE) gel. After transfer, nitrocellulose membranes were blotted with the following antibodies: anti-Rho mAb (Upstate Biotechnology), mouse anti-pMLC2 (Cell Signaling Technology), rabbit anti-MLC2 (Santa Cruz Biotechnology, Santa Cruz, CA), rat anti-Hsc70 (Stressgen, Victoria, BC, Canada), and mouse anti–β-actin (Sigma, St Louis, MO). Primary antibodies were revealed with appropriate secondary antibodies conjugated with horseradish peroxidase and the filters were developed with an enhanced chemiluminescence (ECL) system (ECL detection kit, Amersham, Orsay, France).

Platelet activation analysis

CD34$^+$ cells isolated from leukapheresis were cultured in serum-free medium with TPO. Then, 10 μg/mL Rho inhibitor Tat-C3, 50 μM myosin light chain kinase inhibitor peptide 18 (P18), or 10 μM ROCK inhibitor Y27632 (Calbiochem, Darmstadt, Germany) was added at day 10 of culture. Platelet activation by thrombin was performed at day 11 as described previously.[27] Normal peripheral blood platelets were used as control. Briefly, cultured cells were stimulated for 10 minutes at 37°C with 2 U/mL thrombin (Stago Diagnostica, Asnières sur Seine, France) added directly to the culture well. Activated and nonactivated platelets were incubated for 30 minutes with both rabbit anti–CD62-PE and mouse anti–CD41a-FITC (Becton Dickinson, le Pont de Claix, France). Platelets were then fixed for 1 hour with an equal volume of 0.5% paraformaldehyde

and suspended in PBS; samples were analyzed with a FACSsort cytometer and the Cell Quest software package (Becton Dickinson).

Electron microscopy

$CD34^+$ cells isolated from leukapheresis were cultured in serum-free medium with TPO. At day 11, the cells were harvested 24 hours after addition of the different inhibitors. The cells were fixed with 1.25% glutaraldehyde in 0.1 mM phosphate buffer for 1 hour at room temperature, washed, postfixed with osmium tetroxide, dehydrated, and embedded in Epon (TAAB, Aldermaston, Berkshire, United Kingdom). Thin sections were examined with a Philips CM 10 electron microscope (Philips, Eindhoven, The Netherlands) after uranyl acetate and lead citrate staining. Platelet large axis (a) and small axis (b) were measured on electron micrographs; their surface was compared to an ellipse and calculated as: $s = \pi ab$. Fifteen platelets were measured in each condition.

Confocal microscopy

Cover glasses of 17 mm were mounted on slides using a drop of Vectashield hard set mounting medium (Vector, Burlingame, CA). Stacks of confocal images were collected with a Zeiss LSM 510 laser scanning confocal microscope (Carl Zeiss, Oberkochen, Germany) using a 63×/1.4 NA oil-immersion Apochromat Plan objective lens. Z-protection of slices and image analyses were performed using Zeiss Image Examiner software.

Results

Rho expression during MK differentiation

$CD34^+$ cells derived from leukapheresis were cultured in liquid serum-free medium supplemented with TPO to induce MK differentiation. As previously reported,[27] MK differentiation in this system is partially synchronous with most MKs being immature before day 7 and with maturation occurring from day 7 to day 9. In this culture system stimulated with TPO, the percentage of MKs on day 9 exceeds 75%.[27] Platelet shedding begins on day 10 and, usually, peaks at day 12. Rho expression was analyzed by costaining with an anti-VWF polyclonal antibody and an anti-Rho mAb. Confocal microscopy revealed that Rho was expressed in VWF-negative cells (probably corresponding to immature MKs, data not shown), mature VWF-positive MKs (Figure 1Ai-iv) as well as MKs forming PPTs (Figure 1Av-vi). Rho was diffusely distributed in the cytoplasm. However, in some MKs, Rho was clearly localized along the plasma membrane suggesting that Rho is activated in some cultured MKs (Figure 1Aiii-iv). To measure Rho expression during MK differentiation, Western blot analyses were performed on whole cultures of $CD34^+$-derived cells at day 3 and on $CD41^+$ cells at days 6, 9, and 12. As compared to Hsc70 used as a control for protein loading, the Rho protein was expressed at an almost constant level during MK differentiation (Figure 1B).

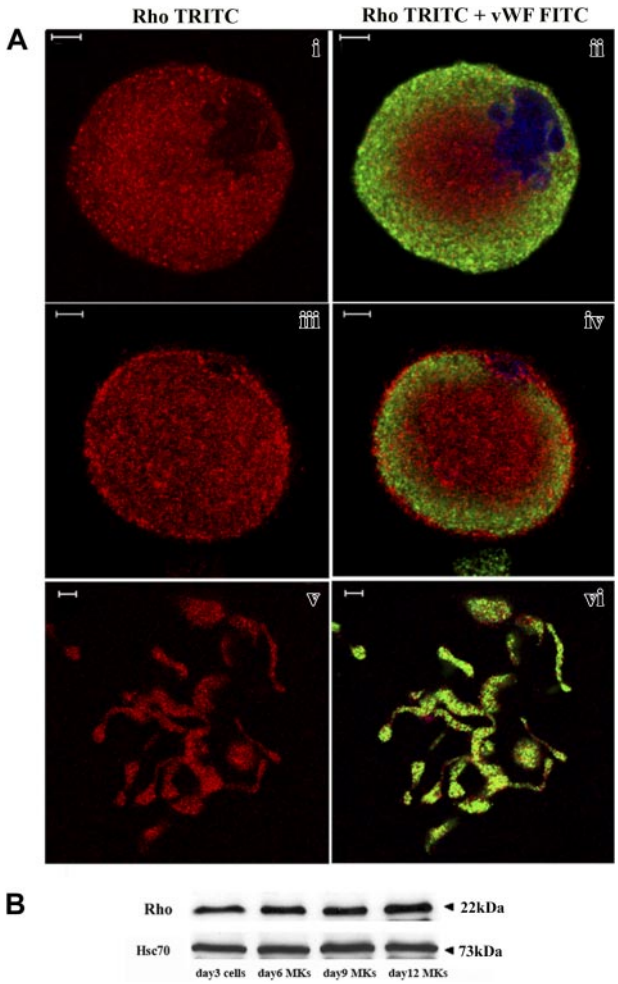

Figure 1. Rho expression during MK differentiation. $CD34^+$ cells purified from blood leukapheresis were cultured in the presence of TPO. At day 6 and day 12 of culture, cells were dually stained with a VWF polyclonal antibody (green) and an anti-Rho mAb (red). (A) Rho was uniformly distributed all over the cytoplasm of mature MKs with a slight reinforcement along the plasma membrane (i-ii). Rho was distributed clearly along the plasma membrane in another MK suggesting an activation site (iii-iv). In MKs forming PPTs, Rho was localized all over the cytoplasm (v-vi). Bars represent 5 μm. (B) The level of Rho was studied by Western blotting using Hsc70 as the control. At day 3, Western blots were performed on total culture. In contrast, at days 6, 9, and 12, Western blots were performed with $CD41^+$MKs.

TPO activates Rho in a differentiation-regulated manner

Pull-down analyses were performed to determine Rho activity during in vitro megakaryopoiesis. The GST-RBD (Rhotekin Rho-binding domain) was used to immunoprecipitate the active Rho-GTP form. Cytokine-deprived $CD41^+$ MKs were stimulated by TPO from 5 to 120 minutes. After an overnight starvation, a residual Rho activity was found both in immature MKs collected at day 7 and in more mature MKs collected at day 12. Nevertheless, Rho could be further activated in response to TPO stimulation both in immature (day 7) and more mature (day 12) MKs (Figure 2A). Rho activity peaked at 5 minutes. The band intensities of active Rho (Rho-GTP) and total Rho were quantified by densitometry. Quantification results show that TPO-stimulated Rho activity measured at 5 minutes was decreased about 22% at day 12 compared to day 7 (Figure 2B). This decrease in Rho activity was confirmed in 3 independent experiments. These results indicate that the TPO/Mpl signaling is implicated in Rho activation during megakaryopoiesis and that Rho activation by TPO appears to be slightly down-regulated during MK differentiation.

Rho activation inhibits PPF

To investigate the role of Rho during MK differentiation, we used retroviral constructs encoding active or dominant-negative forms of RhoA. Two MKs sources were infected by these retroviruses: MKs derived from cord blood $CD34^+$ cells that were cultured 6 days with TPO and SCF and MKs derived from mobilized $CD34^+$ cells that were cultured during 3 days with a mixture of cytokines (TPO, SCF, IL-3, FLT3-L). MK populations expressing GFP ($CD41^+GFP^+$) were sorted by flow cytometry 48 hours after infection and seeded at 20×10^3 cells/mL in serum-free liquid medium in the presence of TPO. The percentage of MKs bearing

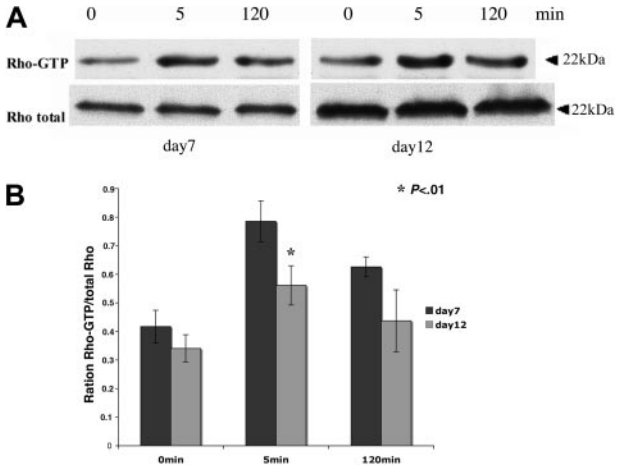

Figure 2. Rho activity can be stimulated by TPO during MK differentiation. CD41$^+$ MKs derived from leukapheresis were cytokine-starved overnight in serum-free medium and then stimulated for 5 minutes and 120 minutes with 100 ng/mL TPO. Pull-down RBD-bound Rho and total Rho in the lysate were detected by Western blot. (A) Cultured MKs starved on day 6 and stimulated on day 7 (left panel) or starved on day 11 and stimulated on day 12 (right panel). (B) Western blot quantification showing the Rho-GTP/total Rho ratio at day 7 and day 12 of culture. Results are the average ± SD of 3 experiments. The same number of cells were used for pull-down analysis at day 7 and day 12 of culture. In this experiment, the total quantities of Rho augmented from day 7 to day 12 because the MK size markedly increases in culture during this time lapse. Thus, the ratio between Rho-GTP and total Rho permits evaluation of the relative activity of Rho. Quantification results show that TPO-stimulated Rho activity measured at 5 minutes decreased of about 22% at day 12 compared to day 7 (*t* test; $P < .01$).

PPTs was quantified daily under an inverted microscope. The presence of at least one pseudopodial extension was considered as PPT. Three independent experiments were performed with each MKs source and results are illustrated in Figure 3A-B. Whether MKs were derived from cord blood or leukapheresis CD34$^+$ cells, overexpression of RhoAN19 led to an increase in PPF as compared to the Migr control. In contrast, overexpression of RhoAV14 induced a 2- to 3-fold decrease in PPF that remained significant during the time course of the study. The representative micrographs to generate Figure 3B are illustrated in Figure 3C. These data suggest that Rho activation could inhibit PPF.

Adhesion of primary human MKs onto fibrillar collagen I substrate induces Rho activation and stress fiber formation.[26] To evaluate the functionality of our constructs, MKs derived from leukapheresis CD34$^+$ cells were infected and selected as described. CD41$^+$GFP$^+$ cells were then cultured in liquid serum-free medium supplemented with TPO for one additional day and allowed to adhere during 1 hour onto collagen I to enumerate MKs showing stress fibers. Stress fiber assembly was seen in 30.7% MKs infected with the empty vector (Migr-GFP$^+$), 42.7% Migr-RhoAV14-GFP$^+$ MKs, and 20.4% Migr-RhoAN19-GFP$^+$ MKs (Figure 4B). Strikingly, only thin stress fibers with faint actin filament bundles were observed in Migr-RhoAN19-GFP$^+$ MKs; in contrast, stress fibers seen in Migr-RhoAV14-GFP$^+$ MKs were much thicker and more obvious than in the control (Figure 4A). These results demonstrate that overexpression of RhoAV14 or RhoAN19 was functional in altering the actin cytoskeleton.

Status of MLC2 phosphorylation during MK differentiation

One major role of the Rho/ROCK pathway is to regulate the actin/myosin motor by modifying the MLC2 phosphorylation status. To examine the localization of pMLC2 during MK differentiation, cultures derived from leukapheresis CD34$^+$ cells were dually stained with fluorescent-conjugated anti–phospho-MLC2 and anti-VWF antibodies. Confocal microscopy revealed that pMLC2 was present in the cytoplasm in both mature or less mature MKs identified on VWF expression (Figure 5Ai-iv). In some MKs, pMLC2 was relatively abundant in the cell cortex (data not shown). In MKs forming PPTs, pMLC2 was also localized along the cytoplasm extensions (Figure 5v-vi, arrow 1) with the predominance in the swellings (arrows 4 and 5) and the tips of PPTs (arrows 2 and 3).

We then analyzed the expression of total MLC2 and pMLC2 (Ser19) on whole cultures of CD34$^+$-derived cells at day 3 and purified CD41$^+$MKs at days 6, 9, and 12. In 3 independent experiments, both total MLC2 and pMLC2 increased during MK differentiation (Figure 5B). Strikingly, the increase in pMLC2 level was greater than the rise of total MLC2 protein level (Figure 5C-D). Quantification of the band intensities by densitometry showed that pMLC2 augmented rapidly between day 3 (total culture) and day 9 when MK polyploidization occurred in culture, whereas the increase became much slighter between day 9 and day 12 when PPT formation started (Figure 5C-D). Noteworthy, β-actin expression level also increased during differentiation (Figure 5B).

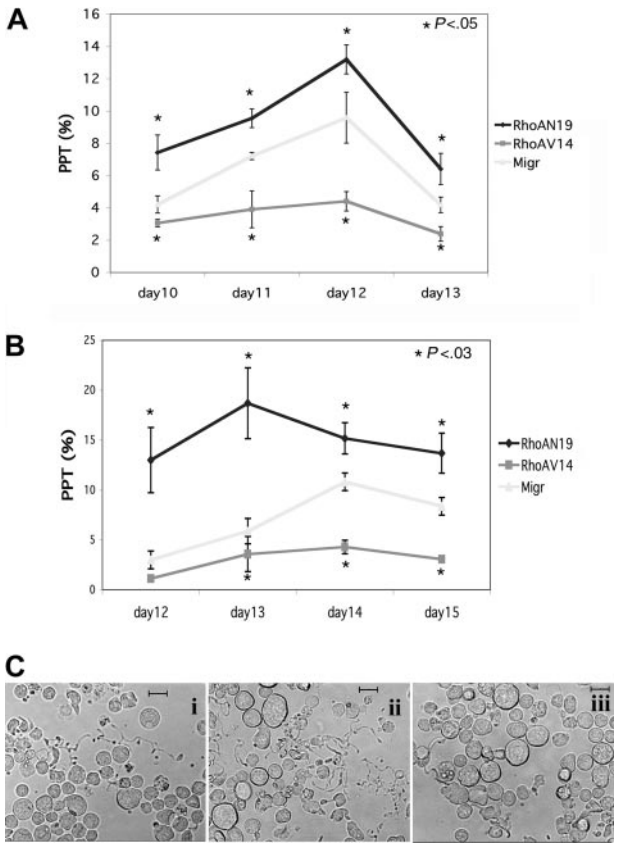

Figure 3. Differential effect of RhoAN19 and RhoAV14 overexpression on PPF. CD41$^+$ MKs derived from CD34$^+$ cells from leukapheresis or umbilical cord blood were infected either with Migr-GFP$^+$ or Migr-RhoAV14-GFP$^+$ or Migr-RhoAN19-GFP$^+$. At 48 hours after infection GFP$^+$ MKs were selected and then cultured. The effects of the constructs were studied on PPF. On the day indicated, the percentage of MKs exhibiting at least one PPT extension was determined by counting at least 300 MKs in each experimental group. Results are expressed as the mean ± SD of 3 independent experiments. (A) CD41$^+$ MKs derived from leukapheresis CD34$^+$ cells where PPF was scored every day from day 10 to day 13. Calculated percentages for each time point were 4.2%, 7.2%, 9.6%, and 4.2% for control Migr-GFP; 7.4%, 9.6%, 13.2%, and 6.4% for RhoAN19; and 3.1%, 3.9%, 4.4%, and 2.4% for RhoAV14 (*t* test; $P < .05$). (B) CD41$^+$ MKs derived from umbilical cord blood CD34$^+$ cells where PPF was scored every day from day 12 to day 15. Calculated percentages for each time point were 3%, 5.9%, 11.5%, and 8.3% for control Migr-GFP; 12.9%, 18.7%, 15.1%, and 13.7% for RhoAN19; and 1.1%, 3.5%, 4.3%, and 3% for RhoAV14 (*t* test; $P < .03$). (C) Representative micrographs of MKs derived from cord blood CD34$^+$ at day 13: i, Migr-GFP$^+$; ii, Migr-RhoAN19-GFP$^+$; iii, Migr-RhoAV14-GFP$^+$. Bars represent 20 μm.

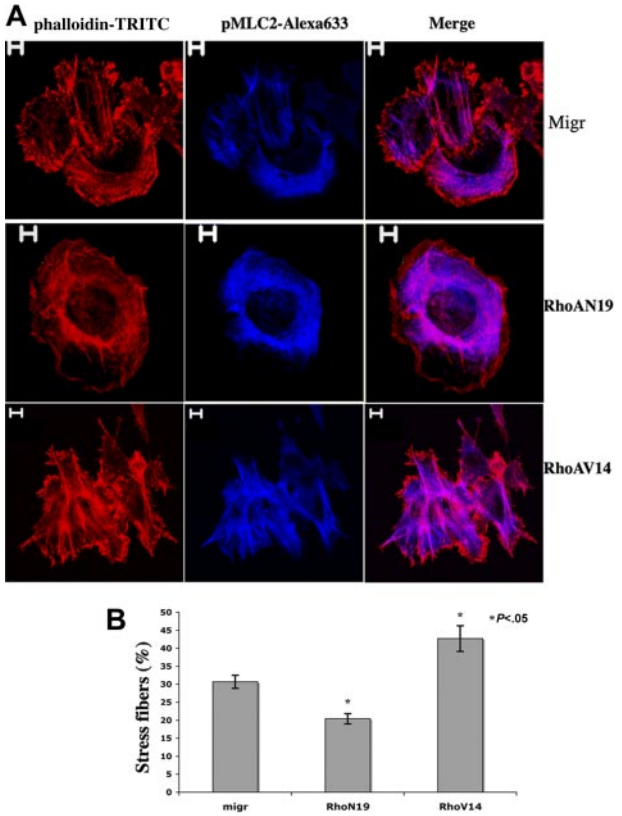

Figure 4. Differential effects of RhoAN19 and RhoAV14 overexpression on fiber stress formation induced by collagen I. (A) Migr-GFP$^+$, Migr-RhoAV14-GFP$^+$, and Migr-RhoAN19-GFP$^+$ MKs were plated onto collagen I substrate for 1 hour on day 6, and cells were dually stained with a pMLC2 mAb (blue) and phalloidin-TRITC (red). Bars represent 5 μm. (B) The graph illustrates the mean percentage ± SD of Migr-GFP$^+$, Migr-RhoAV14-GFP$^+$, and Migr-RhoAN19-GFP$^+$ MKs showing stress fibers after 1 hour of adhesion onto collagen I. At least 300 cells were counted in 3 separate experiments. Stress fiber assembly was induced in 30.7% MKs infected with the empty vector (Migr-GFP$^+$), 42.7% Migr-RhoAV14-GFP$^+$ MKs, and 20.4% MKs infected with Migr-RhoAN19-GFP$^+$.

Rho, ROCK, and MLCK inhibitors decrease MLC2 phosphorylation while increasing PPF

To investigate whether Rho/ROCK inhibits PPF by regulating MLC2 phosphorylation, a Rho inhibitor (Tat-C3) or a ROCK inhibitor (Y27362) or a selective inhibitor of MLCK (P18)[29] was added at day 9 or day 10 in culture of CD41$^+$ cells derived from leukapheresis when full MKs cytoplasmic maturation was observed. PPTs were quantified 24 hours after addition of the compounds. Three independent experiments were performed. Inhibition of Rho, ROCK, and MLCK led to a significant increase in PPT count as shown in Figure 6A. Moreover, the combined addition of ROCK and MLCK inhibitors had an additive effect on PPF.

At the same time, Western blot analyses were also performed with CD41$^+$ MKs after 24 hours of treatment with Tat-C3, Y27362, or P18. A partial inhibition of MLC2 phosphorylation was found with all 3 compounds. However, the inhibition with P18 was more marked than with Tat-C3 and Y27632. Furthermore, the effects of P18 and Y27632 on the level of MLC2 phosphorylation were additive (Figure 6B). Taken together, these results suggest that MLC2 phosphorylation plays a key role in PPF and that MLC2 phosphorylation is partly regulated by the Rho/ROCK pathway.

Structure and function of PPTs or platelets produced in the presence of the Rho/ROCK pathway inhibitors

CD34$^+$ cells isolated from leukapheresis were cultured in serum-free medium with TPO and platelets were collected at day 11, 1 day after addition of one of the 3 inhibitors in culture. Platelets derived from cultures containing one of the 3 inhibitors were increased in size and exhibited α- and dense granules (Figure 7A). Their mean surfaces, as estimated on thin sections, were respectively: 4.0 ± 1.0 μm^2 (Tat-C3); 4.1 ± 3.0 μm^2 (Y27362); 4.9 ± 5.1 μm^2 (P18), consistently larger than the one of platelets produced in the control conditions (2.3 ± 1.9 μm^2). Some platelets produced in the

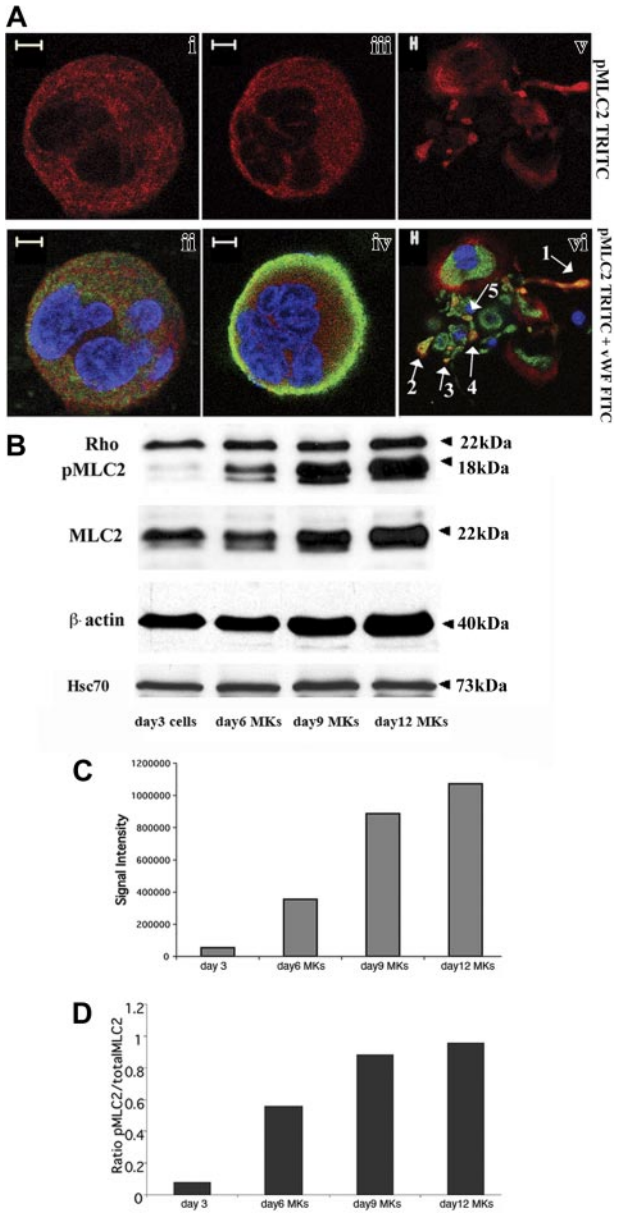

Figure 5. MLC2 phosphorylation status during megakaryocyte differentiation. (A) Immunolabeling was performed with an anti-pMLC2 (red), an anti-VWF (green), and a TOTO-3 iodide (blue). Photomicrographs were taken using a Zeiss laser scanning microscope equipped with a 63×/1.4 numerical aperture (NA) oil objective. pMLC2 was localized in the cytoplasm of immature (i-ii) and mature MKs (iii-iv). In MK-forming PPTs (v-vi), pMLC2 was localized along the cytoplasmic extensions (arrow 1), in the swellings (arrows 4 and 5), and in the tips of PPTs (arrows 2 and 3). Bars represent 5 μm. (B) CD34$^+$ cells derived from leukapheresis were cultured 3 days with TPO, and one part of the cells was collected. Culture was continued, and CD41$^+$ MKs were selected at day 5 as described in "Materials and methods" and grown for additional days with TPO. Western blots were performed on cells collected on day 3 and on MKs collected on days 6, 9, and 12. β-Actin, MLC2, and pMLC2 protein levels increased from day 3 to day 12. Rho was expressed at an almost constant level regardless of the MK differentiation stages. Anti-Hsc70 antibody was used as a control of protein loading. (C-D) Western blot quantification showed the increase in both pMLC2 (C) and pMLC2/MLC2 ratio (D) during MK differentiation.

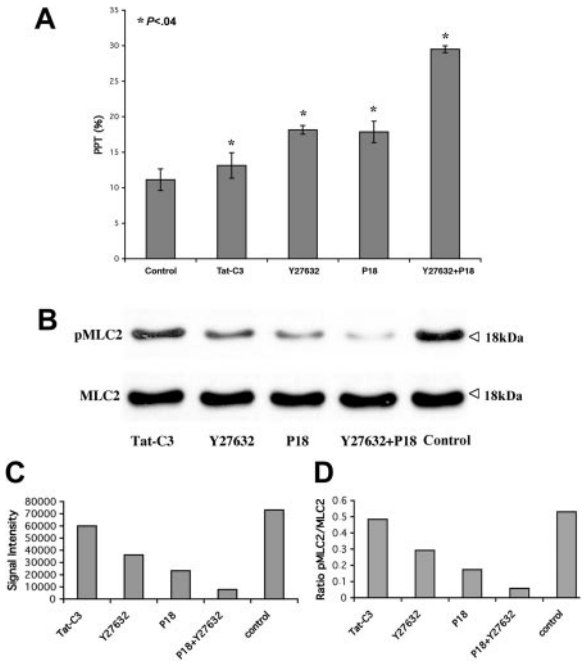

Figure 6. Inhibition of Rho, ROCK, and MLCK decreases MLC2 phosphorylation while increasing PPF. The Rho inhibitor Tat-C3 (10 μg/mL), ROCK inhibitor Y27632 (10 μM), or MLCK inhibitor P18 (50 μM) alone or in combination with Y27632 was added at day 10 to CD41$^+$ MKs derived from leukapheresis. (A) PPT quantification on day 11 showing a significant increase of PPT with all these inhibitors. Three independent experiments were performed (*t* test; $P < .04$). Error bars indicate SD. (B-D) Western blot performed on the CD41$^+$ MKs treated for 24 hours either with Tat-C3, Y27632, or P18 showing a partial inhibition of pMLC2. An additive effect was observed in combination P18 with Y27632.

presence of Y27632 were adherent but did not exhibit any ultrastructural evidence of activation. No marked difference was observed in the demarcation membrane system of MKs treated with the different inhibitors.

Immunofluorescence labeling performed with an anti-VWF polyclonal antibody and an antitubulin mAb revealed a normal distribution of VWF and microtubule coils in the vast majority of PPTs produced with or without the different inhibitors (data not shown).

Finally, we tested whether the different inhibitors modify platelet activation by studying CD62 (P-selectin) on the surface of the platelets released in culture. Using flow cytometry, we considered platelets produced in vitro as CD41$^+$ elements with similar scatter properties as blood platelets. Before thrombin addition, the level of CD62 on the platelet surface was low in each condition demonstrating further that none of these compounds induced platelet activation. When thrombin (2 U/mL) was added for 5 minutes, the activation response of platelets produced with the inhibitors was similar to the response obtained with control platelets suggesting that the inhibitors did not alter platelet functions (Figure 7B).

Discussion

The molecular mechanisms leading to platelet release in the blood flow are still incompletely understood. Platelet biogenesis depends on the formation of long and thin cytoplasm extensions called PPTs. Such extensions are under the control of cytoskeleton reorganizations that play an important role in PPT elongation, PPT amplification, and platelet release. It has been reported that PPT elongation is regulated by microtubules, whereas actin is involved in the branching structures that lead to amplification and render platelet shedding more efficient. We have previously reported that PPF was impaired in MKs adherent onto collagen I and we have suggested that this inhibition was related to the Rho/ROCK pathway.

Herein, we provide direct evidence that the Rho/ROCK pathway, a well-defined regulator of actin dynamics, acts as a negative regulator of PPF. This conclusion was reached by 2 main experiments: first, overexpression of a dominant-negative Rho (RhoAN19) led to an increase in PPF, whereas overexpression of a spontaneously active Rho (RhoAV14) inhibited PPF; second, inhibition of the Rho/ROCK pathway by the specific Tat-C3 or Y27632 compounds resulted in a marked increase in PPF. In addition, our data suggest that inhibition of PPF by the Rho/ROCK pathway likely occurs through MLC2 phosphorylation. This conclusion is supported by the significant increase of PPTs in the presence of either Tat-C3 or Y27632 both of which inhibited MLC2 phosphorylation. Moreover, in the presence of P18, a MLCK inhibitor, MLC2 phosphorylation was also inhibited and PPF increased. MLC2 phosphorylation at Ser19 is mainly regulated by 2 different kinases: ROCK and MLCK. As the key effectors of Rho, ROCK (especially isoform ROCK II) promotes MLC2 phosphorylation by 2 mechanisms: it phosphorylates the myosin-binding subunit (MBS) of the myosin phosphatase thereby inhibiting its phosphatase activity and also directly phosphorylates MLC2 at Ser19.[17-20] MLCK, a Ca^+/calmodulin-dependent kinase, is the major kinase that phosphorylates MLC2 at Ser19.[22,30,31] Thus, MLC2 phosphorylation depends on a balance between myosin phosphatase and MLCK activation. The effects of the MLCK inhibitor on MLC2 phosphorylation were more important than those of the ROCK inhibitor in mature MKs. This result is consistent with previous reports showing that platelets contain much lower amounts of ROCK than MLCK and that MLC2 phosphorylation is regulated by both ROCK and MLCK during platelet activation.[22,23] However, we cannot exclude the

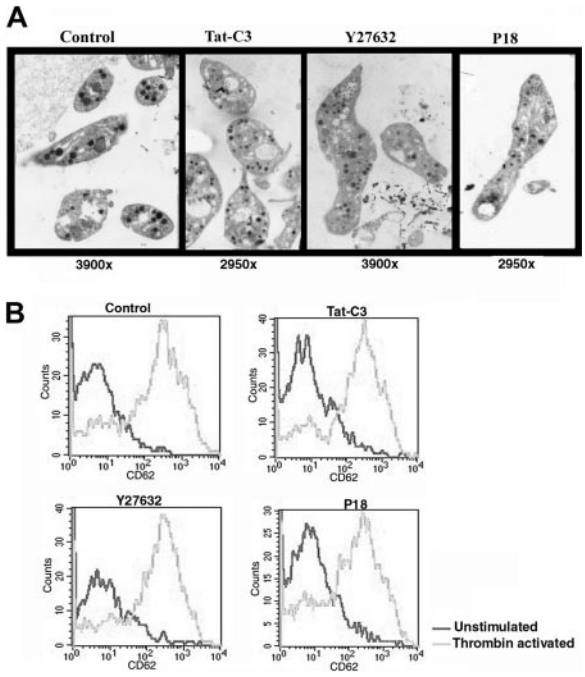

Figure 7. Structure and function of platelets produced in vitro in the presence of inhibitors of the Rho/ROCK pathway. (A) Platelets obtained with Y27632 or Tat-C3 or P18 display a normal ultrastructure under electron microscopy but an increased size compared to the untreated control. (B) Platelets produced in serum-free medium with or without inhibitors were activated by thrombin (2 U/mL) and analyzed by flow cytometry. Platelets produced with all 3 inhibitors display a normal response to thrombin activation.

possibility that other Rho/ROCK effectors might be implicated in the negative regulation of PPF such as LIM kinase, which can inactivate cofilin, an actin depolymerizing protein.[32-34]

In contrast to our previous report in which MKs were allowed to adhere onto matrix-coated slides, we used here a suspension serum-free liquid culture devoid of cell/matrix interactions. In this system, TPO alone could activate Rho, but the level of activation slightly decreased in the mature stages. The link between Mpl signaling and Rho activation is poorly known and will require further studies. Nevertheless, our data imply that, during MK differentiation, cell autonomous changes in the TPO-mediated Rho activation must occur to allow PPF. Likewise, we have evidence that TPO activation of the MAP kinase/ERK pathway, a pathway also involved in the inhibition of PPF, is down-regulated at the end of MK maturation (N.D., personal results). Thus, these data suggest that some signaling pathways activated by TPO/Mpl are alleviated at the end of MK maturation allowing PPF.

Increasing evidence indicates that Rho/ROCK stimulates the contractile activity of actin/myosin, accelerates membrane retraction,[15,16,35] and, thus, may inhibit a pseudopodial process. In contrast, studies performed with fibroblasts have indicated that Cdc42 and Rac, 2 other major members of the Rho GTPase family, promote membrane protrusion. The fibroblast model has been used extensively to explain the effects of Rho, Rac, and Cdc42 in neurite outgrowth and differentiation. Rac and Cdc42 signaling promotes neurite formation, whereas Rho activation antagonizes this effect and causes neurite retraction.[16,36,37] According to the neurite model, it can be speculated that Rac or Cdc42 may provide protrusion forces in MKs leading to PPF, whereas Rho/ROCK through MLC2 phosphorylation would generate opposite forces restraining cytoplasmic extensions. During the early stages of maturation, Rho activation predominates and thus restricts PPF. At the end of maturation, the decline in Rho activation or presumably an increase in Cdc42 activation allows an advantage to protrusion forces leading to PPF. Therefore, when the Rho/ROCK pathway was inhibited between day 10 and day 11, which corresponds to the onset of PPF in cultured MKs, the opposite force equilibrium in MKs was disrupted and led to an increase in PPF. Supporting this hypothesis, a recent work has shown that a dominant-negative N-WASp repressed PPF by inhibiting local assembly of actin fibers along demarcation membranes.[13] Our ongoing studies aiming to address the role of Cdc42 and Rac in PPF show that an overexpression of a dominant-negative Cdc42 (Cdc42N17) strongly inhibited PPF, whereas overexpression of a spontaneously active Cdc42 (Cdc42V12) led to an increase in PPF (data not shown).

The fact that we observed a similar increase in expression levels of actin, phospho-MLC2, and total MLC2 all along MK differentiation raises another important question: What is the role of the actin/myosin motor during MK differentiation? The increased expression may be directly related to the marked enlargement in MK size after endomitosis because actin/myosin activation is strongly implicated in cell volume response, during cell swelling and shrinkage.[38,39] To rapidly adapt to the cell volume augmentation and to keep a normal shape, MKs probably need to enhance actin/myosin activity to provide more contractility. The parallel increase between actin and phospho-MLC2 suggests that actin/myosin contractility may be needed to keep a normal cell shape during polyploidization and to impair premature PPT formation. Another role of MLC2 phosphorylation may be related to PPT constrictions and platelet shedding. This assumption is based on the observation that phospho-MLC2 was localized along the cytoplasmic extension, especially in swellings and tips of PPTs. It was shown that PPTs could develop segmented constrictions along their length that impart a beaded appearance (swelling). Then, with a rapid retraction, PPT strands were separated from residual nuclear mass.[10] Here, we suppose that actin/myosin motor could supply contractility for both constrictions and retraction of PPTs. When pMLC2 was inhibited, platelet size was increased in absence of enough contractile force. Together, the data suggest that pMLC2 may have 2 opposite roles: one at the beginning of platelet biogenesis possibly by impairing the unfolding of demarcation membranes[13] and an opposite role by regulating platelet release and size. These results suggest that both the level and the localization of pMLC2 might be tightly regulated during megakaryopoiesis.

Interestingly, at least 2 human platelet disorders associated with an increased platelet size may be due to defects in actin/myosin activation.[40] The Bernard-Soulier syndrome is associated with an absence or a deficient expression of the GPIb-GPIX-GPV complex that is linked to the membrane actin cytoskeleton and may participate in cytoskeletal transduction signaling leading to normal platelet formation. The May-Hegglin syndrome is a rare inherited human macrothrombocytopenia caused by an inactivating mutation in the nonmuscle myosin heavy-chain 9 gene *(MYH9)*. MYH9 encodes the heavy chain of nonmuscle myosin IIA (NMMHC-IIA) that is the only myosin isoform present in platelets. A myosin II molecule is composed of 2 heavy chains, each of which is associated with 2 MLC2 chains. Myosin heavy chain contains an ATPase activity and MLC2 phosphorylation is essential for myosin activation.[31,41] The precise effects of the *MYH9* mutations on myosin functions are controversial and the way they lead to macrothrombocytopenia has not been documented.[42] Nevertheless, it has been hypothesized that the defect in platelet production is linked to an abnormal PPT formation because both MKs numbers in bone marrow and platelet clearance were normal.[43]

Altogether, the present report shows for the first time that inhibition of MLC2 phosphorylation by either Tat-C3 or Y27632 or P18 increases PPF but these PPTs were abnormal and associated with an increased size in the produced platelets. These data suggest that the regulation of pMLC2 probably plays a critical role in the formation of normal-sized platelets and may prevent disorganized cytoplasmic extension.

Acknowledgments

This work was supported by grants from INSERM, la Ligue Nationale Contre le Cancer (équipes labellisées 2004 and 2007; W.V. and J.B.) and Agence Nationale de la Recherche (Blanc).

Y.C. received postdoctoral training grants from la Ligue Nationale Contre le Cancer and from the ANR (ANR Blanc). F.A. received postdoctoral training grants from la Ligue Nationale Contre le Cancer.

We want to express our gratitude to Françoise Wendling for carefully reviewing the manuscript. We acknowledge Eric Cao for technical help.

Authorship

Conflict-of-interest disclosure: The authors declare no competing financial interests.

Correspondence: Najet Debili, INSERM U790, Institut Gustave Roussy, 39 rue Camille Desmoulins, 94805, Villejuif, France; e-mail: denali@igr.fr.

References

1. Gewirtz AM. Megakaryocytopoiesis: the state of the art. Thromb Haemost. 1995;74:204-209.
2. Zimmet J, Ravid K. Polyploidy: occurrence in nature, mechanisms, and significance for the megakaryocyte-platelet system. Exp Hematol. 2000;28:3-16.
3. Radley JM, Scurfield G. The mechanism of platelet release. Blood. 1980;56:996-999.
4. Hartwig J, Italiano J Jr. The birth of the platelet. J Thromb Haemost. 2003;1:1580-1586.
5. Cramer EM, Norol F, Guichard J, et al. Ultrastructure of platelet formation by human megakaryocytes cultured with the Mpl ligand. Blood. 1997; 89:2336-2346.
6. Patel SR, Hartwig JH, Italiano JE. The biogenesis of platelets from megakaryocyte proplatelets. J Clin Invest. 2005;115:3348-3354.
7. Italiano JE Jr, Bergmeier W, Tiwari S, et al. Mechanisms and implications of platelet discoid shape. Blood. 2003;101:4789-4796.
8. Schwer HD, Lecine P, Tiwari S, Italiano JE Jr, Hartwig JH, Shivdasani RA. A lineage-restricted and divergent beta-tubulin isoform is essential for the biogenesis, structure and function of blood platelets. Curr Biol. 2001;11:579-586.
9. Lecine P, Italiano JE Jr, Kim SW, Villeval JL, Shivdasani RA. Hematopoietic-specific beta 1 tubulin participates in a pathway of platelet biogenesis dependent on the transcription factor NF-E2. Blood. 2000;96:1366-1373.
10. Italiano JE Jr, Lecine P, Shivdasani RA, Hartwig JH. Blood platelets are assembled principally at the ends of proplatelet processes produced by differentiated megakaryocytes. J Cell Biol. 1999; 147:1299-1312.
11. Rojnuckarin P, Kaushansky K. Actin reorganization and proplatelet formation in murine megakaryocytes: the role of protein kinase c alpha. Blood. 2001;97:154-161.
12. Fox JE. Cytoskeletal proteins and platelet signaling. Thromb Haemost. 2001;86:198-213.
13. Schulze H, Korpal M, Hurov J, et al. Characterization of the megakaryocyte demarcation membrane system and its role in thrombopoiesis. Blood. 2006;107:3868-3875.
14. Schwartz M. Rho signalling at a glance. J Cell Sci. 2004;117:5457-5458.
15. Raftopoulou M, Hall A. Cell migration: Rho GTPases lead the way. Dev Biol. 2004;265:23-32.
16. Etienne-Manneville S, Hall A. Rho GTPases in cell biology. Nature. 2002;420:629-635.
17. Amano M, Ito M, Kimura K, et al. Phosphorylation and activation of myosin by Rho-associated kinase (Rho-kinase). J Biol Chem. 1996;271: 20246-20249.
18. Kimura K, Ito M, Amano M, et al. Regulation of myosin phosphatase by Rho and Rho-associated kinase (Rho-kinase). Science. 1996;273:245-248.
19. Kawano Y, Fukata Y, Oshiro N, et al. Phosphorylation of myosin-binding subunit (MBS) of myosin phosphatase by Rho-kinase in vivo. J Cell Biol. 1999;147:1023-1038.
20. Kureishi Y, Kobayashi S, Amano M, et al. Rho-associated kinase directly induces smooth muscle contraction through myosin light chain phosphorylation. J Biol Chem. 1997;272:12257-12260.
21. Sebbagh M, Renvoize C, Hamelin J, Riche N, Bertoglio J, Breard J. Caspase-3-mediated cleavage of ROCK I induces MLC phosphorylation and apoptotic membrane blebbing. Nat Cell Biol. 2001;3:346-352.
22. Bauer M, Retzer M, Wilde JI, et al. Dichotomous regulation of myosin phosphorylation and shape change by Rho-kinase and calcium in intact human platelets. Blood. 1999;94:1665-1672.
23. Suzuki Y, Yamamoto M, Wada H, et al. Agonist-induced regulation of myosin phosphatase activity in human platelets through activation of Rho-kinase. Blood. 1999;93:3408-3417.
24. Nakai K, Suzuki Y, Kihira H, et al. Regulation of myosin phosphatase through phosphorylation of the myosin-binding subunit in platelet activation. Blood. 1997;90:3936-3942.
25. Watanabe Y, Ito M, Kataoka Y, et al. Protein kinase C-catalyzed phosphorylation of an inhibitory phosphoprotein of myosin phosphatase is involved in human platelet secretion. Blood. 2001; 97:3798-3805.
26. Sabri S, Jandrot-Perrus M, Bertoglio J, et al. Differential regulation of actin stress fiber assembly and proplatelet formation by alpha2beta1 integrin and GPVI in human megakaryocytes. Blood. 2004;104:3117-3125.
27. Norol F, Vitrat N, Cramer E, et al. Effects of cytokines on platelet production from blood and marrow $CD34^+$ cells. Blood. 1998;91:830-843.
28. Chagraoui H, Komura E, Tulliez M, Giraudier S, Vainchenker W, Wendling F. Prominent role of TGF-beta 1 in thrombopoietin-induced myelofibrosis in mice. Blood. 2002;100:3495-3503.
29. Lukas TJ, Mirzoeva S, Slomczynska U, Watterson DM. Identification of novel classes of protein kinase inhibitors using combinatorial peptide chemistry based on functional genomics knowledge. J Med Chem. 1999;42:910-919.
30. Kohama K, Ye LH, Hayakawa K, Okagaki T. Myosin light chain kinase: an actin-binding protein that regulates an ATP-dependent interaction with myosin. Trends Pharmacol Sci. 1996;17:284-287.
31. Sellers JR, Pato MD. The binding of smooth muscle myosin light chain kinase and phosphatases to actin and myosin. J Biol Chem. 1984; 259:7740-7746.
32. Maekawa M, Ishizaki T, Boku S, et al. Signaling from Rho to the actin cytoskeleton through protein kinases ROCK and LIM-kinase. Science. 1999;285:895-898.
33. Ohashi K, Nagata K, Maekawa M, Ishizaki T, Narumiya S, Mizuno K. Rho-associated kinase ROCK activates LIM-kinase 1 by phosphorylation at threonine 508 within the activation loop. J Biol Chem. 2000;275:3577-3582.
34. Sumi T, Matsumoto K, Nakamura T. Specific activation of LIM kinase 2 via phosphorylation of threonine 505 by ROCK, a Rho-dependent protein kinase. J Biol Chem. 2001;276:670-676.
35. Jaffe AB, Hall A. Rho GTPases: biochemistry and biology. Annu Rev Cell Dev Biol. 2005;21:247-269.
36. Van Aelst L, Cline HT. Rho GTPases and activity-dependent dendrite development. Curr Opin Neurobiol. 2004;14:297-304.
37. Govek EE, Newey SE, Van Aelst L. The role of the Rho GTPases in neuronal development. Genes Dev. 2005;19:1-49.
38. Eggermont J. Rho's role in cell volume: sensing, strutting, or signaling? Focus on "Hyperosmotic stress activates Rho: differential involvement in Rho kinase-dependent MLC phosphorylation and NKCC activation." Am J Physiol Cell Physiol. 2003;285:C509–511.
39. Di Ciano-Oliveira C, Sirokmany G, Szaszi K, et al. Hyperosmotic stress activates Rho: differential involvement in Rho kinase-dependent MLC phosphorylation and NKCC activation. Am J Physiol Cell Physiol. 2003;285:C555–566.
40. Balduini CL, Iolascon A, Savoia A. Inherited thrombocytopenias: from genes to therapy. Haematologica. 2002;87:860-880.
41. Weiss A, Leinwand LA. The mammalian myosin heavy chain gene family. Annu Rev Cell Dev Biol. 1996;12:417-439.
42. Canobbio I, Noris P, Pecci A, Balduini A, Balduini CL, Torti M. Altered cytoskeleton organization in platelets from patients with MYH9-related disease. J Thromb Haemost. 2005;3:1026-1035.
43. Hamilton RW, Shaikh BS, Ottie JN, Storch AE, Saleem A, White JG. Platelet function, ultrastructure, and survival in the May-Hegglin anomaly. Am J Clin Pathol. 1980;74:663-668.